First real-time measurement of the evolving H-2/H-1 ratio during water evaporation from plant leaves

Kerstel, ERT; van der Wel, LG; Meijer, HAJ

Published in:
Isotopes in Environmental and Health Studies

DOI:
10.1080/10256010500230007

Isotopes in Environmental and Health Studies
Vol. 41, No. 3, September 2005, 207–216

Taylor & Francis
Taylor & Francis Group

First real-time measurement of the evolving $^{2}H/^{1}H$ ratio during water evaporation from plant leaves

ERIK R. T. KERSTEL*, L. GERKO VAN DER WEL and HARRO A. J. MEIJER

CIO – Center for Isotope Research, University of Groningen, Nijenborgh 4,
9747 AG Groningen, The Netherlands

(Received 13 April 2005; in final form 22 June 2005)

We have studied the temporal behaviour of the deuterium isotope ratio of water vapour emerging from a freshly cut plant leaf placed in a dry nitrogen atmosphere. The leaf material was placed directly inside the sample gas cell of the stable isotope ratio infrared spectrometer. At the reduced pressure (~40 mbar) inside the cell, the appearance of water evaporating from the leaf is easily probed by the spectrometer, as well as the evolving isotope ratios, with a precision of about 1 ‰. The demonstration experiment we describe measures the $^{2}H/^{1}H$ isotope ratio only, but the experiment can be easily extended to include the $^{18}O/^{16}O$ and $^{17}O/^{16}O$ isotope ratios. Plant leaf water isotope ratios provide important information towards quantification of the different components in the ecosystem water and carbon dioxide exchange.

Keywords: Deuterium; Isotope ratio infrared spectrometry; Plant leaf water; Spectroscopy; Water vapour

1. Introduction

Measurement of the isotopic composition of bulk plant leaf water, as well as that of the vapour phase in the immediate vicinity of the leaf, is important for two principal reasons: (1) they provide essential information for the understanding of plant physiology (see, e.g. [1–3]), and (2) oxygen atoms are efficiently exchanged between plant leaf water and atmospheric carbon dioxide, accompanied by a characteristic isotope fractionation [4]. Therefore, to understand the ^{18}O signal in CO_2, knowledge of the isotopic make-up of – the different reservoirs within – plant leaf water is a prerequisite (see, e.g. [5] and references therein). The total CO_2 flux from biosphere to atmosphere depends on two processes: CO_2 respiration from the soil and the photosynthetic CO_2 assimilation and (photo)respiration of the plants. Partitioning of the two fluxes is possible by measuring the $^{18}O/^{16}O$ isotope ratio and comparing it to the value of ecosystem water. In both soil and plant leaves, the presence of the carbonic anhydrase enzyme ensures that the $^{18}O/^{16}O$ isotopic equilibrium is reached quickly. The relatively enriched plant leaf water causes a high $^{18}O/^{16}O$ isotope ratio for photosynthetic CO_2 [1], whereas

*Corresponding author. Tel.: +31-50-3634-759; Fax: +31-50-3634-738; Email: e.r.t.kerstel@rug.nl

Isotopes in Environmental and Health Studies
ISSN 1025-6016 print/ISSN 1477-2639 online © 2005 Taylor & Francis
http://www.tandf.co.uk/journals
DOI: 10.1080/10256010500230007

the ^{18}O depleted soil water leads to a low $^{18}O/^{16}O$ value for soil respired CO_2 [6–8]. Yet, quantification of these reservoirs appears to be a difficult task, both from a model and an experimental perspective. This lack of knowledge hampers the use of the $\delta^{18}O$ isotope signal in atmospheric CO_2 (co-registered with $\delta^{13}C$ since the late 1970s on many sites) for improving the quantitative knowledge of the carbon cycle [9, 10].

Until recently, water isotope ratio studies had to rely on isotope ratio mass spectrometry (IRMS). This technique has already benefited from over 40 years of commercial development, and instrumentation can be bought which is able to attain very high levels of precision, in combination with a high throughput. However, three major drawbacks exist: (1) since the instrumentation is not compatible with condensable gases, chemical conversion of the water sample is needed to produce H_2 and CO_2 (or CO or O_2) for measurement of the hydrogen or oxygen isotope ratios, respectively. (2) Nearly always, the sample needs to be 'extracted' from the system being studied. Furthermore, the discrete character of the measurements forces investigators to study the process of their choice with 'grab samples' instead of following it (semi-)continuously and in real-time. In addition, the sampling reduces the temporal resolution, which thus becomes a limiting factor in many ecological or eco-physiological applications. (3) Finally, a number of practical problems confine the use of an IRMS apparatus to a dedicated laboratory and exclude application 'in the field'. Most notable are the high capital and maintenance cost, the size ($>1\,m^3$), weight ($>500\,kg$) and power consumption of the apparatus and the necessity of operation by a trained technician.

For some of the same reasons mentioned earlier, we started almost 10 years ago with the development of a novel, laser-based technique for the measurement of water isotope ratios. In this technique, which we call stable isotope ratio infrared spectrometry (SIRIS), the infrared spectrum is used to obtain quantitative information on the isotope ratios of a gas phase sample. Most small molecules exhibit highly characteristic rotational–vibrational bands in this 'finger print' region. The corresponding spectra are highly sensitive to isotopic substitution of the molecule and can be recorded by measuring the intensity decrease of a laser beam that has traversed several meters through a water vapour as a function of the laser wavelength. The absorption features in these spectra can be uniquely assigned to one of the water isotopologues (including $H^{16}OH$, $H^{17}OH$, $H^{18}OH$ or $H^{16}O^2H$), whereas the Beer–Lambert law relates the laser intensity loss to the corresponding isotopologue number density. In this way, we can determine the relative deviation of the isotope ratio in the sample with respect to the same ratio in the reference material (*i.e.*, the delta value) by recording two spectra, one belonging to the sample and the other to a known reference material.

Our early work has been carried out using an isotope ratio spectrometer with a colour centre laser (FCL, from the German *Farbe*) as light source [11]. This laser is very broadly tunable in the 3-μm region, where most small molecules exhibit strongly absorbing fundamental vibrational bands. At present, we use almost exclusively III–V type DFB diode lasers near 1.4 μm. The lower absorption strength of the overtone vibrational bands that are excited in this case is easily compensated for by a more sensitive wavelength modulation detection technique and better infrared detector performance.

The internal precision of our laser measurements of the $^2H/^1H$ isotope ratio is currently about 0.5 ‰ and about a factor of 2 better for the oxygen isotopes [12]. This is comparable to measurements with IRMS. A major advantage of the SIRIS method is the direct measurement on water vapour without any (chemical) pre-treatment of the sample. Moreover, all three isotope ratios of interest, $^2H/^1H$, $^{17}O/^{16}O$ and $^{18}O/^{16}O$, can be measured simultaneously on one and the same sample. The measurement of ^{17}O via the CO_2 equilibrium method is impossible with IRMS (due to the mass-overlap with the more abundant ^{13}C in CO_2). In addition, the measurement is non-destructive: in principle, the sample can be recovered. Furthermore, a major advantage of SIRIS is the possibility to build compact, lightweight and energy efficient instrumentation (especially when using near-infrared diode lasers), for

in situ and real-time monitoring applications. These are obvious advantages when it comes to carrying out, for example, ecological field studies.

$^{18}O/^{16}O$ measurements have been recently reported in ecological water samples, using a modified version of the Campbell Scientific isotope ratio optical spectrometer [13]. This commercial instrument uses a Pb-salt laser and MCT detector, which both require liquid nitrogen cooling. In principle, it could also measure $^2H/^1H$, but its precision in this case is insufficient for any practical application. Two other water isotope ratio optical spectrometers have been described [14, 15], but both of these were developed for the study of extremely dry air masses in or near the stratosphere. These instruments are extremely sensitive, but less precise and accurate than the instruments considered here, that all use multiple-pass absorption cells to achieve a sufficiently high sensitivity with a relatively simple experimental configuration.

In this article, we demonstrate the potential of our 'simple' near-infrared isotope ratio spectrometer for eco-physiological studies by measuring real-time the behaviour of the water vapour, indicated by the $^2H/^1H$ ratio, emerging from a freshly cut plant leaf placed in a dry nitrogen atmosphere, directly inside the sample gas cell of the spectrometer.

2. Experimental set-up

The experimental set-up used for this experiment differs only in details from that previously described in depth [12, 16]. Figure 1 shows a schematic representation of the experimental setup.

Briefly, the instrument is equipped with two single-mode, thermo-electrically cooled diode lasers. These lasers can be used in a wavelength multiplexing arrangement, enabling the simultaneous registration of two spectral ranges (each about 1.5 cm^{-1} wide) [12]. The first probes, besides a $H^{16}OH$ spectral feature, lines assigned to $H^{17}OH$, $H^{18}OH$ and $H^{16}O^2H$, near 7184 cm^{-1} (1.392 μm). The second laser probes $H^{18}OH$ and $H^{16}O^2H$ (and, of course, again a $H^{16}OH$ line) near 7200 cm^{-1} (1.389 μm), or only $H^{16}O^2H$ and $H^{16}OH$ near 7198 cm^{-1}, but with a better overall performance on the deuterium isotope determination. In this study, only the second laser was used, near 7198 cm^{-1}. This was done to optimize the performance on the δ^2H determination, as the leaf isotope signals were expected to be most pronounced for the deuterium isotope. After passing through an optical isolator and a long focal length lens, a 50 % beam splitter produces two nearly equal intensity beams that are each coupled

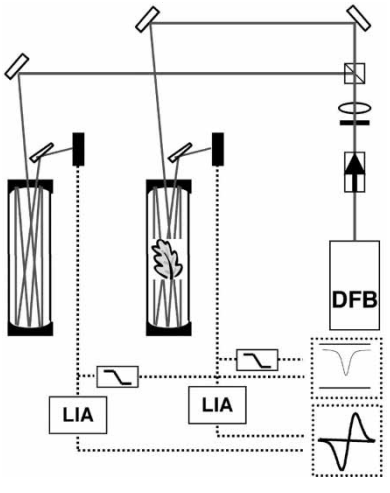

Figure 1. Schematic representation of the experimental setup showing the diode laser source (DFB), the multiple-pass gas cells, optical detectors, low-pass filters and lock-in amplifiers (LIA).

into a different (but identical) home-built multiple pass cell of the Herriot type [17]. The base length of the cells is 43 cm, yielding an effective optical absorption path length of 20.5 m after 48 passes between the two spherical mirrors inside the cell. Initially, both cells are filled with dry nitrogen to a pressure of 40 mbar. One cell provides a reference spectrum. A reference water material, 10 µl liquid water, directly back-traceable to the international standard material Vienna Standard Mean Ocean Water (VSMOW), is injected through a silicon septum into the cell with a volume of about 1 l. The δ^2H-value of the local reference water (known as GS-48) is -43.3 ‰ with respect to VSMOW. The water partial pressure in the cell remains well below the saturation pressure and complete evaporation of the reference material is assured. For the purpose of the experiments described here, the second, sample, cell was equipped with a small pyrex chamber with a volume of about 25 cc. The freshly cut leaf material was quickly transferred to this chamber under a dry-nitrogen atmosphere, after which a valve was opened to connect the small chamber to the larger gas cell volume (with 40 mbar dry N_2). At this point, the data collection was started. In the current configuration, we can record and store one spectrum (*i.e.*, one isotope ratio measurement) in about 14 s. In this case, five spectra were averaged, before calculating the $^2H/^1H$ isotope ratio. Including overhead, this translates in a little over one isotope ratio measurement in 90 s, resulting in a very good temporal coverage of the slowly varying isotope signals. It should be noted that although the primary signals are recorded by wavelength modulation of the laser and phase-sensitive (lock-in) detection, we also record the low-pass detector signals, which show the power tuning curve of the laser as it is injection-current tuned over the spectrum, with superimposed the direct absorption signals of each gas cell. Figure 2 shows typical sample and reference spectra before averaging. The signal-to-noise ratio on the strongest line ($H^{16}OH$) exceeds 10,000, whereas for the weaker line ($^2H^{16}O^1H$), this ratio is about one order of magnitude smaller. As expected, the wavelength modulation signals (modulation index is about 2) closely resemble the first derivative of the absorption line profile [18].

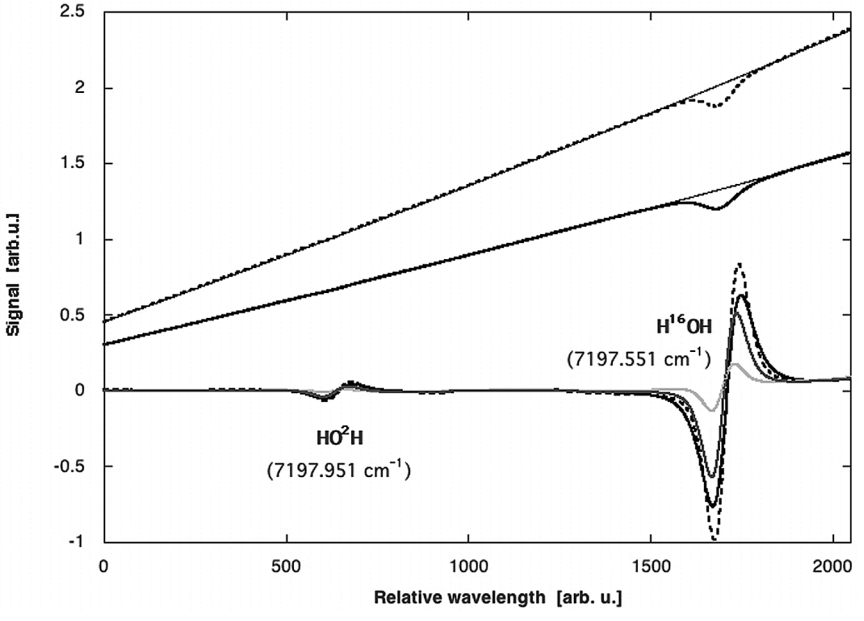

Figure 2. Typical wavelength modulation (bottom) and direct absorption signals (top). The dotted curves are the reference cell spectra, whereas the solid curves give the sample cell spectra at three different times. For clarity, the direct absorption curves are given only for the last measurement. Clearly visible is the increase in signal strength with continuing evaporation of sample water. Barely visible in the spectra, at the scale of the figure, are two weak HO^2H absorptions in between the two marked lines that are used for the deuterium isotope analysis.

Immediately before and following each measurement series (typically lasting 3 h), the gas cells (both reference and sample) were repeatedly flushed with dry nitrogen and (re-)evacuated.

The intensity of the recorded lines is temperature sensitive. This is because the intensity depends not only on the number density of the absorbing molecules but also on the line strength. The effect on the measured isotope ratio can be shown, to a high degree of accuracy, to be sensitive to the temperature *difference* between the reference and sample [19]. For the spectral lines used in this study, the sensitivity is about 7.5 ‰ K^{-1}. Through simple passive temperature stabilization of the two cells together, this potential error source can be easily kept within the precision of the measurement (*i.e.*, <0.5 ‰). This does not account for possibly disturbing effects caused by the temperature dependence of wall adsorption inside the gas cell.

3. Data analysis

In previous experiments, the amount of water vapour was always the same for sample and reference gas cells and constant during the measurements. The algorithm used for the data analysis under these conditions is based on the intensity of the lines and has been described in detail in ref. [11]. In the situation of the present experiment, with highly variable amounts of water vapour in the sample cell, we have instead elected to use the area underneath the absorbance line profile, as it is directly proportional to the number density and independent of any line broadening.

Under the conditions of our experiment, the absorbance line profile is accurately described by a Voigt profile, the convolution of a Gaussian profile (describing Doppler broadening, dominant at low pressure) and a Lorentzian profile (describing pressure broadening). The area belonging to the two selected spectral features is determined by performing a least-squares fit to the line of the first derivative of the Voigt line profile (over a range of ±3 times the Voigt half width at half maximum (hwhm) around the centre line position). The fit returns the height H, Lorentz hwhm (w_L) and Gaussian hwhm (w_G) parameters of the Voigt profile. The area A of the Voigt profile can be now calculated analytically, if one remembers that the area of a given Voigt profile is given by the ratio of its height and the height *NormH* of the corresponding normalized Voigt profile:

$$A(w_L, w_G) = \frac{H(w_L, w_G)}{NormH(w_L, w_G)} \tag{1}$$

It is not difficult to show that the normalized height equals

$$NormH(w_L, w_G) = \left(\frac{\ln 2}{\pi}\right)^{1/2} \frac{1}{w_G} e^{b^2}\, erfc(b) \tag{2a}$$

with:

$$b \equiv (\ln 2)^{1/2} \frac{w_L}{w_G} \tag{2b}$$

So far, we have assumed that the measured spectrum corresponds to the (first derivative of the) absorbance spectrum, for which the intensities (areas) are proportional to the molecular number density. The absorbance α can be related to the absorptance $\Delta I / I_0$ through the Beer law:

$$\alpha = -\ln\left(\frac{I_0 - \Delta I}{I_0}\right) = \frac{\Delta I}{I_0} + \frac{1}{2}\left(\frac{\Delta I}{I_0}\right)^2 + \frac{1}{3}\left(\frac{\Delta I}{I_0}\right)^3 + \cdots \tag{3}$$

In a wavelength modulation experiment, the measured signal is to good approximation proportional to ΔI, but there is no information on I_0, that is, the 100 % transmission level. Without

knowing the ratio of ΔI to I_0, it is impossible to reconstruct the absorbance spectrum reliably. As equation (3) shows, absorbance and absorptance are only linearly related for small values of the absorptance. In our experiment, the absorptance of the $H^{16}OH$ line in the reference cell amounts to 6.5 % and the deviation from linearity is 3.4 %, whereas the absorptance and deviation from linearity are negligibly small for the weaker HO^2H line. Consequently, the wavelength modulation spectrum underestimates the peak absorbance (intensity) of the reference cell $H^{16}OH$ line by 3.4 %, or 34 ‰. At the beginning of the experiment, when still very little water has evaporated into the sample cell, no such error is made with the sample cell $H^{16}OH$ line. The apparent isotope ratio of sample with respect to reference is then ∼34 ‰ lower than the true value. As the sample cell fills with water vapour, the error becomes smaller, until it is zero when the water amount matches that in the reference cell, and eventually changes sign and increases again when more water is present in the sample cell than in the reference cell.

It is for the above that the direct absorption signals (absorptance) are recorded by low-pass filtering of the detector output (to eliminate the high-frequency modulation of the laser power, associated with the wavelength modulation scheme). First of all, to divide the spectra by a smoothed curve representing the changing laser power during an injection-current scan (the thin solid line in figure 2) and, secondly, to be able to apply a first-order correction to the measured δ-value for the non-linear behaviour of the Beer law, according to equation (3).

As the low-pass data is of lower quality than the wavelength modulation spectra, this procedure necessarily adds noise to the δ-values. In addition, determination of the δ-values using the area under the absorbance curves is less precise, although more accurate, than the line-by-line ratio fit used previously. The combined effect is to reduce the precision of the δ^2H determinations to about 1.1 ‰, compared to about 0.5 ‰ determined previously for this spectrometer (and comparable averaging times) [12]. This estimate is based on measurements of an evaporating water droplet, after about one hour, when the droplet has evaporated completely (see figure 3).

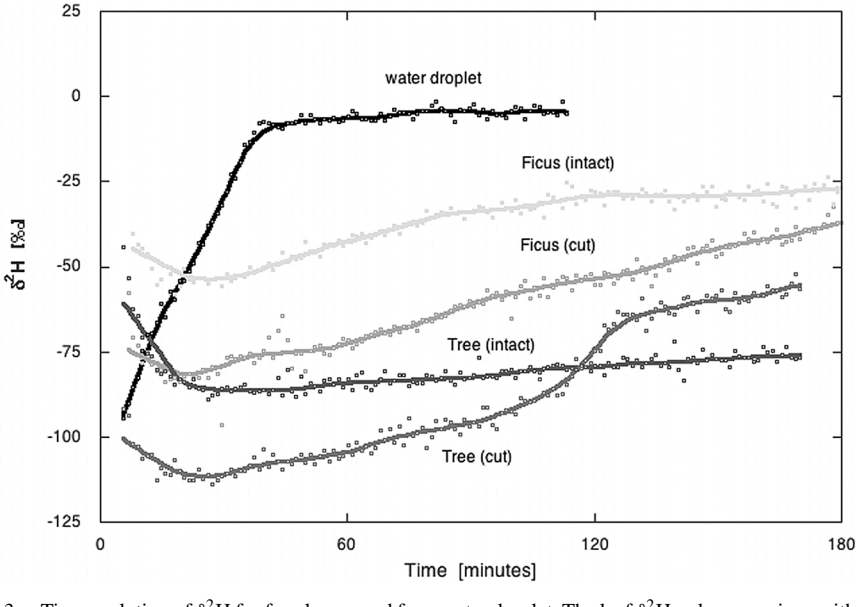

Figure 3. Time evolution of δ^2H for four leaves and for a water droplet. The leaf δ^2H-values are given with respect to the VSMOW international standard material. The δ^2H-value of the droplet is given with respect to the reference cell water ($\delta^2H = -43.3$ ‰ with respect to VSMOW), such that the expected final asymptotic value equals zero. The *Ficus* and tree leaves identified as 'Ficus (cut)' and 'Tree (cut)', respectively, are the leaves that were cut immediately before being transferred to the gas cell.

4. Results and discussion

We have studied the evolving isotope ratios and total water content, following the transfer to the sample gas cell of four pieces of leaf material. Two leaves were taken from a houseplant ('weeping fig', *Ficus benjamina*), two from an unidentified outdoor tree. Of each variety, one leaf was kept intact as much as possible, whereas the other was given a small number of cuts, to possibly facilitate water excretion. As a control experiment, we also once injected a 10 µl droplet of our reference water standard. The results are given in figure 3, which shows the temporal development of the deuterium isotope ratio for water evaporation from the four leaves and the water droplet.

As the $H^{16}OH$ signal strength is a direct measure of the total quantity of water that appeared in the gas phase, we can plot the data of figure 3 also as a function of this evaporated water quantity (as well as the evaporated water quantity as a function of time, data not shown). This is done in figure 4. The latter graph is quite instructive, as it allows us to compare the evaporation of the water droplet to the prediction of a Rayleigh distillation model [20]. The thin solid line in figure 4 represents this model, assuming (incorrectly) that the droplet temperature remains constant at 21 °C. The equilibrium fractionation at this temperature is about −74 ‰. Together with an estimated kinetic fraction of −8 ‰, the combined fractionation used in the model was −82 ‰.

The droplet of reference water nicely shows a Rayleigh-like isotope ratio pattern. The deviation from the model curve is largely due to the drop-in-temperature the droplet immediately after the start of evaporation. The leaf curves show a very different behaviour. Their nearly constant values must either indicate that the total water pool is much larger than the evaporated amount or that mixing within the leaf water pool is minimal and each small evaporating

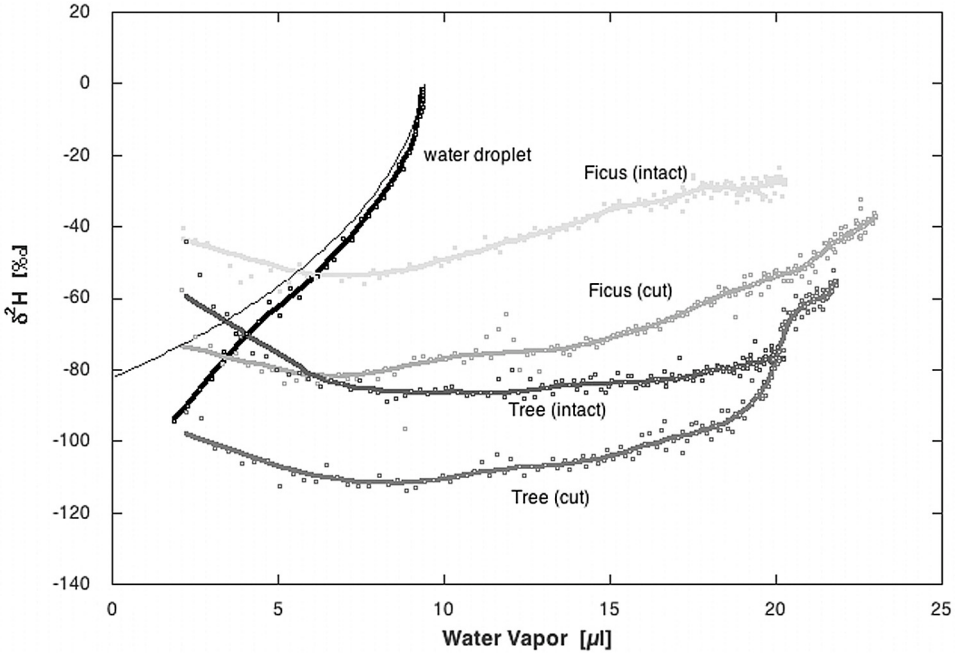

Figure 4. δ^2H as a function of the evaporated water quantity for the four leaves and for the water droplet. The evaporation behaviour of the water droplet is compared to the prediction of a Rayleigh distillation model [20] given by the thin solid line.

portion subsequently evaporates completely, thus without fractionation. In any case, not much difference is observed between the cut and intact leaves. One should keep in mind, however, that in this demonstration experiment, the leaves are brought into a dry, low-pressure nitrogen atmosphere. Although the relative humidity rapidly rises (to a maximum value of roughly 30 %), at no time during the experiment, the pressure rises above 65 mbar. Therefore, firm conclusions about the leaf water pool have to be postponed, until experiments are carried out in which the leaves are kept under more natural conditions.

The data analysis procedure can be improved by carefully linearizing the laser frequency scan, which would improve the quality of the fit to a theoretical line profile. This can be achieved by adding the proper quadratic term to the laser injection current, while monitoring the transmissions of a high resolution etalon. The correction for the non-linear behaviour of the Beer law, now applied to the measured (apparent) δ-value, should be applied to the observed spectra, before the line profile analysis procedure. In addition, the effect of the finite modulation depth on the observed spectrum, and eventually, the measured δ-values, should be investigated in detail. These corrections are expected to be relatively small. However, of more serious concern is the effect of water adsorption on gas cell walls. Fractionation in the adsorption process will tend to make the gas phase water isotopically lighter. In our previous experiments, in which both gas cells were always filled with equal amounts of water, fractionation effects in reference and sample cell would cancel to a high degree in the measured δ-value. The only remaining cause of systematic errors is a memory effect (previous samples affecting the current measurement), which may even be modelled and post-corrected [21]. In the current experiment, with unequal water quantities in the two gas cells, such cancellation would not occur and the resulting fractionation may bias the measurement, whereas the memory effect will slow its time–response. For this reason, we have redesigned the multiple-pass gas cells, eliminating most of the stainless steel surfaces and coating the remaining glass surfaces with a hydrophobic material. These new cells are expected to be soon ready for testing.

5. Conclusion

We have demonstrated the feasibility of following in real-time the isotopic signature of water evaporating from an individual plant leaf. The precision of the δ^2H-measurements is about 1 ‰ (but larger for sample cell water quantities smaller than about 3 µl). The leaves were removed from the plant immediately before the measurement. In the next generation of the spectrometer, we will make a provision to investigate leaves still attached to the plant and the spectrometer will be made much more compact. It now takes up about 1 m^2 on the optical breadboard, whereas the entire spectrometer can easily be housed in a volume of 0.2 m^3 or less.

The time resolution of the measurement can be easily increased to about one measurement per second, of course, at the cost of a lower precision. For example, with a measurement time of 15 s per measurement, we expect precisions better than 2 and 1 ‰ for δ^2H (and δ^{17}O) and δ^{18}O, respectively. Such precisions are still acceptable for the studies proposed here. Moreover, although not shown in these preliminary experiments, the ^{2}H/^{1}H, ^{17}O/^{16}O and ^{18}O/^{16}O ratios can be measured simultaneously, as demonstrated in our earlier work [12, 16]. The measurement of δ^{17}O via the CO_2 equilibrium method is impossible with IRMS (due to mass overlap of ^{17}OCO with the more abundant O^{13}CO), and may be used to study so-called mass independent fractionation effects, or when these are not observed (as is the case for practically all tropospheric water samples), the measurement may be used to increase the precision of the δ^{18}O determination [22].

Instead of measuring the isotope ratios in a static gas cell, the gas of interest could be made to flow through the sample gas cell. Such an approach is used in our stratospheric spectrometer [14] and in the experiment of Lee *et al.* [13]. In contrast to these single cell instruments, the instrument described here is equipped with a separate reference cell, drastically reducing the consumption of (expensive) reference water standards.

Together with the absence of a need for cryogens, the spectrometer is ideally suited for long-term and unattended, *in situ*, ecological field studies.

Acknowledgements

We are grateful to Rolf Siegwolf and Nina Buchmann for helpful discussions and comments on the work presented here. In addition, we thank Janette Spriensma and Henk Been for excellent analytical, respectively, technical support.

References

[1] G.D. Farquhar, J. Lloyd. Carbon and oxygen isotope effects in the exchange of carbon dioxide between plants and the atmosphere. In *Stable Isotope and Plant Carbon/Water Relations*, J.R. Ehleringer, A.E. Hall and G.D. Farquhar (Eds), pp. 47–70, Academic Press, San Diego (1993).

[2] L.A. Cernusak, J.S. Pate, G.D. Farquhar. Diurnal variation in the stable isotope composition of water and dry matter in fruiting *Lupinus angustifolius* under field conditions. *Plant Cell Environ.*, **25**, 893–907 (2002).

[3] B. Barnes, G. Farquhar, K. Gan. Modelling the isotope enrichment of leaf water. *J. Math. Biol.*, **48**, 672–702 (2004).

[4] C.A.M. Brenninkmeijer, P. Kraft, W.G. Mook. Oxygen isotope fractionation between CO_2 and H_2O. *Isot. Geosc.*, **1**, 181–190 (1983).

[5] D. Yakir, L. Sternberg. The use of stable isotopes to study ecosystem gas exchange. *Oecologia*, **123**, 297–311 (2000).

[6] J.R. Gat. Oxygen and hydrogen isotopes in the hydrologic cycle. *Ann. Rev. Earth Planet. Sci.*, **24**, 225–262 (1996).

[7] R. Amundson, L. Stern, T. Baisded, Y. Wang. The isotopic composition of soil and soil respired CO_2. *Geoderma*, **82**, 83–114 (1998).

[8] L. Stern, W.T. Baisden, R. Amunson. Processes controling the oxygen isotopic ratio of soil CO_2: analytic and numerical modelling. *Geochim. Cosmochim. Acta*, **63**, 799–814 (1999).

[9] P. Ciais, A.S. Denning, P.P. Tans, J.A. Berry, D.A. Randall, G.J. Collatz, P.J. Sellers, J.W.C. White, M. Trolier, H.A.J. Meijer, R.J. Francey, P. Monfray, M. Heimann. A three-dimensional synthesis study of ^{18}O in atmospheric CO_2. I. Surface fluxes. *J. Geophys. Res.*, **D 102**, 5857–5872 (1997).

[10] P. Ciais, P.P. Tans, A.S. Denning, R.J. Francey, M. Trolier, H.A.J. Meijer, J. W.C. White, J.A. Berry, D.A. Randall, G.J. Collatz, P.J. Sellers, P. Monfray, M. Heimann. A three-dimensional synthesis study of ^{18}O in atmospheric CO_2. II. Simulations with the TM2 transport model. *J. Geophys. Res.*, **D 102**, 5873–5883 (1997).

[11] E.R.T. Kerstel, R. van Trigt, N. Dam, J. Reuss, H.A.J. Meijer. Simultaneous determination of the $^2H/^1H$, $^{17}O/^{16}O$, and $^{18}O/^{16}O$ isotope abundance ratios in water by means of laser spectrometry. *Anal. Chem.*, **71**, 5297–5303 (1999).

[12] L. Gianfrani, G. Gagliardi, M. van Burgel, E.R.T. Kerstel. Isotope analysis of water by means of near-infrared dual-wavelength diode laser spectroscopy. *Opt. Express* **11**, 1566–1576 (2003).

[13] X. Lee, S. Sargent, R. Smith, B. Tanner. *In situ* measurement of the water vapour $^{18}O/^{16}O$ isotope ratio for atmospheric and ecological applications. *J. Atm. Oc. Techn.*, **22**(5), 555–565 (2005).

[14] E.R.T. Kerstel, H.A.J. Meijer, M. van Burgel, R. Iannone, R. Romanini, J. Morville, L. Gianfrani, G. Gagliardi, H.-J. Jost. Isotope ratio analysis using DFB diode laser spectrometry. In *Proceedings of the 2nd International Symposium on Isotopomers (ISI), November 4–6, 2003 in Stresa, Italy*, C. Guillou and J. Ryder (Eds), pp. 66–69, European Commission, Joint Research Center, Institute for Health and Consumer Protection, Ispra/Varese, Italy, (2004).

[15] C.R. Webster, A.J. Heymsfield. Water isotope ratios D/H, $^{18}O/^{16}O$, $^{17}O/^{16}O$ in and out clouds map dehydration pathways. *Science*, **302**, 1742–1745 (2003).

[16] E.R.T. Kerstel, G. Gagliardi, L. Gianfrani, H.A.J. Meijer, R. van Trigt, R. Ramaker. Determination of the $^2H/^1H$, $^{17}O/^{16}O$, and $^{18}O/^{16}O$ isotope ratios in water by means of tunable diode laser spectroscopy at 1.39 μm. *Spectrochim. Acta*, **A 58**, 2389–2396 (2002).

[17] D.R. Herriott, H. Kogelnik, R. Kompfner. Off-axis paths in spherical interferometers. *Appl. Opt.*, **3**, 523–526 (1964).

[18] J.A. Silver. Frequency-modulation spectroscopy for trace gas detection: theory and comparison among experimental methods. *Appl. Opt.*, **31**, 707–717 (1992).

[19] E.R.T. Kerstel. Isotope ratio infrared spectrometry. In *Handbook of Stable Isotope Analytical Techniques*, P.A. de Groot (Ed.), Chapter 34, pp. 759–787, Elsevier, Amsterdam (2004).
[20] W.G. Mook. *Environmental Isotopes in the Hydrological Cycle: Principles and Applications, Vol. I.* (2001). Available on-line at: http://www.iaea.or.at/programmes/ripc/ih/volumes/volume1.htm.
[21] M. Gehre, H. Geilmann, J. Richter, R.A. Werner, W.A. Brand. Continuous flow $^{2}H/^{1}H$ and $^{18}O/^{16}O$ analysis of water samples with dual inlet precision. *Rapid Commun. Mass Spectrom.*, **18**, 2650–2660 (2004).
[22] R. van Trigt, H.A.J. Meijer, A.E. Sveinbjornsdottir, S.J. Johnsen, E.R.T. Kerstel. Measuring stable isotopes of hydrogen and oxygen in ice: the Bølling transition in the Dye-3 (south Greenland) ice core. *Ann. Glaciol.*, **35**, 125–130 (2002).